

Atom Transfer Processes in Oxidative Quenching of Triplet State Tetrakis(μ -pyrophosphite- P,P')diplatinate(II) by Acidopentacyanocobaltate(III) Anions

Alexander D. Kirk*[†] and Le-Zhen Cai[‡]

Department of Chemistry, University of Victoria, P.O. Box 3065, Victoria, BC, Canada, V8W 3V6, and Delphi Energy and Engine Management Systems, P.O. Box 502650, Indianapolis, Indiana 46250

Received August 29, 1997

In the presence of high electrolyte concentration to screen the Coulomb repulsion, the emission of ${}^3\text{Pt}_2(\text{pop})_4^{4-}$ (where pop = μ -pyrophosphite- P,P') can be quenched by the complexes $\text{Co}(\text{CN})_5\text{X}^{3-}$ (where X = I, Br, Cl, N_3). In acidic aqueous solutions the quenching involves the eventual reduction of the cobalt complexes to $\text{Co}^{2+}_{\text{aq}}$ and gives the oxidative quenching products $\text{Pt}_2^{\text{III}}(\text{pop})_4\text{X}_2^{4-}$ (X = I, Br, Cl). For the reaction of ${}^3\text{Pt}_2(\text{pop})_4^{4-}$ with $\text{Co}(\text{CN})_5\text{I}^{3-}$ and $\text{Co}(\text{CN})_5\text{Br}^{3-}$ in 0.5 M KCl/pH 2 solution, the product yields per quenching event are 0.34 and 0.21, respectively. Steady-state photolysis using the $\text{Co}(\text{CN})_5\text{I}^{3-}$ quencher in 0.5 M KCl medium gave predominantly $\text{Pt}_2(\text{pop})_4\text{I}_2^{4-}$ as product with only small amounts of $\text{Pt}_2(\text{pop})_4\text{ICl}^{4-}$, pointing to a direct iodine atom-transfer process. In contrast, $\text{Co}(\text{CN})_5\text{Br}^{3-}$ quencher gave $\text{Pt}_2(\text{pop})_4\text{Cl}_2^{4-}$ under the same conditions, possibly indicative of electron transfer. However, study of the mixed-valence platinum dimer intermediates formed by laser flash transient spectroscopy provides conclusive evidence for atom transfer as the dominant primary reactive quenching step for all three halopentacyanocobaltates. The steady-state results for $\text{Co}(\text{CN})_5\text{Br}^{3-}$ quencher arose via the interconversion of the monobromo mixed-valence platinum dimer intermediate to its chloro analogue in chloride solutions. $\text{Co}(\text{CN})_5\text{N}_3^{3-}$ gave a mixture of oxidation products and no intermediate corresponding to electron transfer, indicating a complex interaction with ${}^3\text{Pt}_2(\text{pop})_4^{4-}$.

Introduction

There is considerable interest^{1,2} in the photoinduced reactions of metal dimer species such as $\text{Pt}_2(\text{pop})_4^{4-}$ (pop = μ -pyrophosphite- P,P'). This molecule has a long-lived triplet excited state, which phosphoresces with high quantum yield, and can participate in a variety of energy- and electron-transfer processes, with reports^{3–5} of atom-transfer processes in reaction with organic halides. We have recently reported⁶ that this excited triplet state is also quenched by a series of anionic Co(III) complexes, where because of the 3–/4– charge repulsion, the quenching is assisted by electrolyte. The effect of electrolyte concentration on the quenching rate constant was shown to be predicted well by the extended Debye–Hückel theory even up to electrolyte concentrations as high as 2 M. In addition, large specific cation effects were found using different electrolytes and these were interpreted in terms of direct participation of the cation in the transition state for the quenching. The results for different $\text{Co}(\text{CN})_5\text{X}^{3-}$ implied that there were some differences in the mechanism of the quenching for different X, and the present work was undertaken to try to establish the primary quenching process for the four complexes with X = I, Br, Cl,

N_3 . In an earlier communication,⁷ we presented our finding that $\text{Co}(\text{CN})_5\text{I}^{3-}$ represents the first metal complex showing an atom-transfer quenching mechanism in its reaction with ${}^3\text{Pt}_2(\text{pop})_4^{4-}$. Here we present additional evidence for this process and our findings for the remaining complexes.

Experimental Section

Preparation of Materials. The complexes $\text{K}_3[\text{Co}(\text{CN})_5\text{X}]$, with X = I, Br, Cl, N_3 , CN, and $\text{K}_4[\text{Pt}_2(\mu\text{-P}_2\text{O}_5\text{H}_2)_4]\cdot 2\text{H}_2\text{O}$ were prepared, purified, and characterized spectroscopically as detailed earlier.⁶ The spectra of the acidopentacyanocobaltates are available as Figure S1 in the Supporting Information.

Electroanalytical Measurements. Differential pulse polarography experiments were performed using a PAR 174A polarographic analyzer, with a static mercury dropping electrode, Ag/AgCl reference electrode, and a shiny platinum wire as a counter electrode in a standard glass polarography cell. The scan parameters were 10 mV s^{-1} ; range, 0 to –1.5 V; amplitude, 50 mV; drop time, 0.5 s; and filter time constant, 0.3 s. Aqueous solutions were 0.10 M in KNO_3 , 0.010 M in HClO_4 , and 5.0×10^{-4} M in $\text{K}_3[\text{Co}(\text{CN})_5\text{X}]$. All solutions were deaerated by nitrogen for 4 min before scanning under a blanket of N_2 . The polarograms were digitized to disk using a Hewlett-Packard 7475A plotter digitizing system (Un-Plot-It, Silk Scientific Inc.). Conventional polarograms were generated by trapezoidal integration (Igor Pro 3.01, Wavemetrics, Inc) of the differential pulse data.

Spectroscopic and Optical Measurements. UV/vis spectra were run on a Cary 1 or 5 UV/vis Spectrophotometer using 0.7 or 1 cm quartz cells. Spectral data were transferred to a Macintosh IICI for evaluation using Igor Pro. The main application was to the treatment of the difference spectra of product mixtures resulting from steady-state photolysis.

* To whom correspondence should be addressed.

[†] University of Victoria.

[‡] Delphi Energy and Engine Management Systems.

- (1) Zipp, A. P. *Coord. Chem. Rev.* **1988**, *84*, 47–83.
- (2) Roundhill, D. M.; Gray, H. B.; Che, C.-M. *Acc. Chem. Res.* **1989**, *22*, 55–61.
- (3) Che, C.-M.; Lee, W.-M.; Cho, K.-C.; Harvey, P. D.; Gray, H. B. *J. Phys. Chem.* **1989**, *93*, 3095–3099.
- (4) Roundhill, D. M.; Dickson, M. K.; Atherton, S. J. *J. Organomet. Chem.* **1987**, *335*, 413–422.
- (5) Roundhill, D. M.; Atherton, S. J. *Inorg. Chem.* **1986**, *25*, 4071–4072.
- (6) Cai, L.-Z.; Kneeland, D. M.; Kirk, A. D. *J. Phys. Chem.* **1997**, *101*, 3871–3879.

- (7) Kirk, A. D.; Cai, L.-Z. *J. Chem. Soc., Chem. Commun.* **1997**, 523–524.

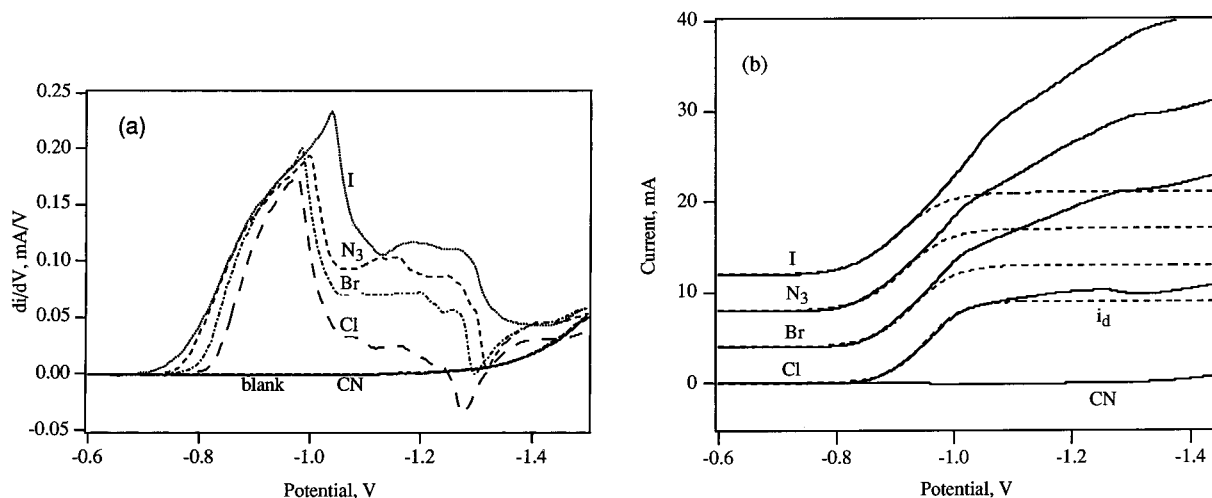


Figure 1. Polarography of 5.0×10^{-4} M $\text{K}_3\text{Co}(\text{CN})_5\text{X}$ ($\text{X} = \text{I}, \text{N}_3, \text{Br}, \text{Cl}, \text{CN}$) in 0.10 M KNO_3 and 0.010 M HClO_4 solution. (a) Differential pulse polarography. (b) Polarographic waves generated from (a) by integration (solid lines) and the computer fittings (dotted lines) based upon eq 1. I, N_3 , and Br waves are offset by 12, 8, and 4 mA, respectively.

Emission spectra were obtained from an Aminco SPF 125 double monochromator spectrofluorometer, using a 1 cm silica fluorescence cell. The light source was a xenon lamp.

Potassium ferrioxalate actinometry^{8–10} was used for measurement of light fluxes. A 3.0 mL aliquot of 0.050 M ferrioxalate solution (0.45 μm filtered) was irradiated for an appropriate time, mixed with 6.00 mL of developer (0.1% 1,10-phenanthroline, 0.75 M sodium acetate in 0.2 M H_2SO_4) and made up to 25.00 mL. After storage in the dark for about 30 min, the $\text{Fe}(\text{phen})_3^{2+}$ product absorbance was measured at 510 nm, where $\epsilon_{510} = 1.105 \times 10^4 \text{ M}^{-1} \text{ cm}^{-1}$. The quantum yield for Fe^{2+} at 360 nm was taken¹¹ to be 1.28.

Steady-State Photolysis. An HBO 100 W mercury lamp was used as the light source for steady-state measurements of quantum yield. The light was filtered through a Corning CS 7–60 filter and a monochromator set at 360 or 365 nm, with 5 cm of water as an infrared absorber. The lamp intensity was 2.4×10^{-9} Einstein s^{-1} . Light intensity was continuously monitored using an Alphametrix model P1110S silicon diode detector and model 1020 m. Solutions were irradiated with nitrogen bubbling in 1 cm rectangular glass spectrophotometer cells held in a thermostated cell compartment at 22.0 ± 0.01 °C. The concentration of $\text{Pt}_2(\text{pop})_4^{4-}$ was typically 3×10^{-5} M, and that of quencher $\text{Co}(\text{CN})_5\text{X}^{3-}$ was in the range $(1-2) \times 10^{-4}$ M, in 0.50 M cation concentration and 0.010 M HClO_4 media. Solutions were photolyzed to conversions less than 15% to avoid secondary photolysis.

Laser Flash Photolysis. Two systems were used. First, a PTI PL 2300 nitrogen laser of pulse energy 1.5 mJ at 337 nm, filtered through a Corning CS 7–54 filter, was wavelength-shifted to 370 nm using a 1 cm cell containing quinine sulfate in ethanol, as previously described.⁷ This was used for lifetime quenching measurements and some of the difference spectral work.

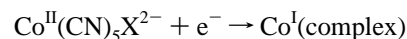
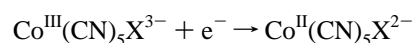
Second, a Spectra-Physics GCR-12 Nd:YAG laser, frequency tripled to 355 nm and used at pulse energy up to 25 mJ, was used for excitation of the sample in a 7.0×7.0 mm Suprasil quartz cell. Transient absorption measurements were made with right angle geometry using an Oriel/Osram 150 W Xe lamp, which can be optionally intensified by pulsing, and a Digichrom 240 computer-controlled monochromator, with appropriate color filters mounted in filter wheels to remove scattered light and unwanted orders. Detection was by a Hamamatsu R928 photomultiplier and Tektronix 520A digital oscilloscope. The system is controlled by a Mac IIsi computer program written using

Labview 3.0 and is capable of transient spectroscopic measurements over the time scale from tens of ns to 0.1 s and the wavelength range 260–800 nm.

Solutions were made up in 1×10^{-3} M HClO_4 aqueous media containing variously 0.5 M KCl, 0.5 M KBr, saturated KClO_4 (~ 0.14 M), and 0.5 M NH_4ClO_4 . Nitrogen was bubbled into all solutions used in this work.

Results

Redox Potential of $\text{K}_3[\text{Co}(\text{CN})_5\text{X}]$ Complexes in Aqueous Acidic Solution. The differential pulse polarograms obtained for the cobalt complexes $\text{K}_3\text{Co}(\text{CN})_5\text{X}$ are shown in Figure 1a. Except for $\text{X} = \text{CN}$, which is difficult to reduce, each complex shows first a very unsymmetrical peak, followed by a poorly defined second reduction, corresponding to irreversible two-step reduction overall. Literature studies of acidopentacyanocobaltate(III) complexes at the dropping mercury electrode^{12,13} similarly concluded that these reductions occur irreversibly in two steps and proposed the following processes:



For an irreversible wave, the estimation of $E_{1/2}$ values is difficult. However, the following modification of the usual equation for the voltammetric potential/current profile has been suggested¹⁴ to apply:

$$E = E_{1/2} + \frac{RT}{\alpha nF} \ln \left\{ \frac{(i_d - i)}{i} \right\} \quad (1)$$

where E , i , i_d , n , R , F , and T have their usual meanings and α is the transfer coefficient ($\alpha = 1$ for a reversible reaction and approaches zero with increasing irreversibility).

To estimate the $E_{1/2}$ values, the normal polarograms were generated by numerical integration (Figure 1b) and fitted to eq 1. Because for an irreversible wave the current rise is slower than for a reversible wave, only the front portions of the polarograms were used to avoid inclusion of part of the second

(8) Hatchard, C. G.; Parker, C. A. *Proc. R. Soc. London, Ser. A* **1956**, 235, 518.
 (9) Parker, C. A. In *Photoluminescence of Solutions*; Elsevier Publishing Co.: Amsterdam, 1968; p 208.
 (10) Kirk, A. D.; Namasivayam, C. *Anal. Chem.* **1983**, 55, 2428–2429.
 (11) Demas, J. N.; Bowman, W. D.; Zalewski, E. F.; Velapoldi, R. A. *J. Phys. Chem.* **1981**, 85, 2766–2771.

(12) Hume, D. N.; Kolthoff, I. M. *J. Am. Chem. Soc.* **1949**, 71, 867–869.
 (13) Maki, N.; Fujita, J.; Tsuchida, R. *Nature* **1959**, 183, 458–459.
 (14) Hibbert, D. B.; James, A. M. *Dictionary of Electrochemistry*, 2nd ed.; The Macmillan Press Ltd.: London, 1984.

Table 1. Estimated Half-Wave Potentials $E_{1/2}$ and Transfer Coefficients (α) for 5.0×10^{-4} M $\text{Co}(\text{CN})_5\text{X}^{3-}$ Complexes (X = I, N_3 , Br, Cl) in 0.10 M $\text{KNO}_3/0.010$ M HClO_4 Aqueous Solution at Room Temperature

X	$E_{1/2}$, V vs Ag/AgCl	$E_{1/2}$, V vs SCE	α	$E_{1/2}$, V vs SCE ¹³
I	-0.90	-0.95	0.65	-0.71
N_3	-0.91	-0.96	0.68	-1.37 ^a
Br	-0.93	-0.98	0.70	-0.71
Cl	-0.95	-1.00	0.80	-0.86

^a Reported for the $2e^-$ reduction process, Co^{III} to Co^{I} .

reduction step. All the $\text{Co}(\text{CN})_5\text{X}^{3-}$ are of the same charge type and similar size, undergo the same reduction process, and were measured under identical conditions, so they should have essentially the same values for the diffusion current (i_d) for the first reduction step. The reduction of the $\text{Co}(\text{CN})_5\text{Cl}^{3-}$ complex shows the least overlap of the second reduction step with the first, so the i_d value obtained from fitting the first wave of the $\text{Co}(\text{CN})_5\text{Cl}^{3-}$ complex was incorporated in the fit of the first waves of the other three complexes, as shown by the dotted fit lines in Figure 1b. This yielded the $E_{1/2}$ values and transfer coefficients given in Table 1. The cyano complex was not reduced before the onset of water reduction, consistent with literature findings.¹³

The $E_{1/2}$ values obtained here are more negative than Makis' results¹³ where 3 M KCl was used as supporting electrolyte and Tween-80 was used as a maximum suppressor. This is consistent with literature observations^{13,15} that the presence of a maximum suppressor (necessary for normal polarography but avoidable in the more accurate differential pulse technique) and the higher concentration of electrolyte would both shift the $E_{1/2}$ positively.

The derived $E_{1/2}$ values and oxidizing abilities are not very different but increase in the order $\text{Co}(\text{CN})_6^{3-} \ll \text{Co}(\text{CN})_5\text{Cl}^{3-} < \text{Co}(\text{CN})_5\text{Br}^{3-} < \text{Co}(\text{CN})_5\text{N}_3^{3-} < \text{Co}(\text{CN})_5\text{I}^{3-}$. When $\text{Co}(\text{III})$ (d^6) is reduced to $\text{Co}(\text{II})$ (d^7), the electron accepted occupies the antibonding e_g orbital which increases in energy with ligand field strength. The $\text{Co}(\text{CN})_6^{3-}$ complex should therefore be the weakest oxidant, and the oxidizing ability should increase as found, with the exception that the azido complex is a somewhat better oxidant than expected.

Reactive Quenching, Products, and Reaction Efficiency.

The acidopentacyanocobaltate have been found⁶ to be efficient quenchers of ${}^3\text{Pt}_2(\text{pop})_4^{4-}$ in the presence of moderate to high concentrations of electrolyte. Hexacyanocobaltate did not quench the ${}^3\text{Pt}_2(\text{pop})_4^{4-}$ emission decay lifetime within experimental error but for the other complexes, the quenching rate constants increased in the order $\text{Co}(\text{CN})_5\text{Cl}^{3-} < \text{Co}(\text{CN})_5\text{Br}^{3-} < \text{Co}(\text{CN})_5\text{N}_3^{3-} < \text{Co}(\text{CN})_5\text{I}^{3-}$. In this work, the nature of the quenching process has been pursued by studies with the iodo-, bromo-, and chloropentacyanocobaltates and found to lead to redox products. Thus when a deaerated solution of $\text{K}_4\text{Pt}_2(\text{pop})_4$, quencher $\text{K}_3\text{Co}(\text{CN})_5\text{X}$ (X = Br, I) and 0.500 M $\text{KY}/0.010$ M HClO_4 (Y = Br, Cl) was irradiated at 370 nm with continuous degassing, the absorption bands of reactant $\text{Pt}_2(\text{pop})_4^{4-}$ at 370 nm and quencher $\text{Co}(\text{CN})_5\text{X}^{3-}$, in the region of 250–270 nm were bleached in a 1:2 molar ratio, Figures 2–4. This was accompanied by the development of new bands, which comparison with literature spectra shows can be attributed to $\text{Pt}_2(\text{pop})_4\text{X}_2^{4-}$, $\text{Pt}_2(\text{pop})_4\text{Y}_2^{4-}$, and possibly some $\text{Pt}_2(\text{pop})_4\text{XY}^{4-}$. The reactions terminated when the light source was removed, indicating that neither thermal nor photocatalytic reactions contribute to the photochemical reaction.

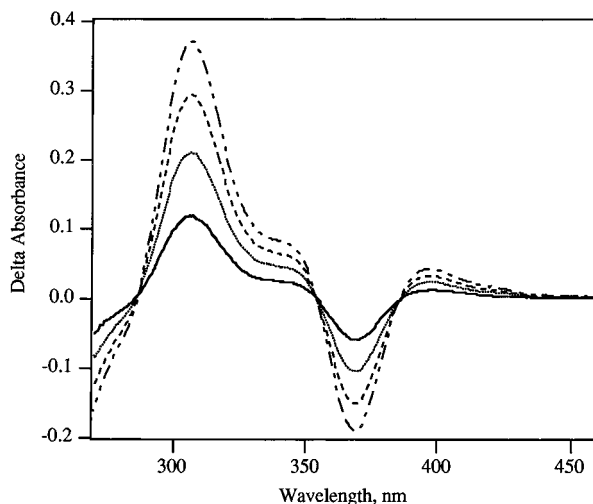


Figure 2. Absorbance changes on photoreaction of ${}^3\text{Pt}_2(\text{pop})_4^{4-}$ with $\text{Co}(\text{CN})_5\text{Br}^{3-}$ in 0.50 M $\text{KBr}/0.010$ M HClO_4 aqueous solution. N_2 laser, shifted to $\lambda_{\text{irrad}} = 370$ nm. Numbers of pulses are (—) 60, (···) 120, (---) 180, (- - - -) 240.

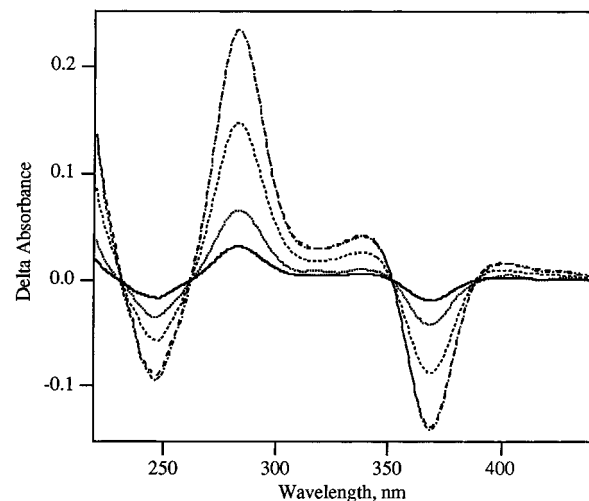


Figure 3. Absorbance changes on photoreaction of ${}^3\text{Pt}_2(\text{pop})_4^{4-}$ with $\text{Co}(\text{CN})_5\text{Br}^{3-}$ in 0.50 M $\text{KCl}/0.010$ M HClO_4 aqueous solution; Hg lamp, irradiation times: 30 s (—); 60 s (···); 120 s (---); 180 s (- - -); and kept in dark for 180 s after the last irradiation (---) (last two coincide).

When X = Y = Br, the absorption bands developed at 307, 345, and 395 nm, as shown by the differential absorption spectra for increasing light exposures of Figure 2. The photoproduct was identified by the peak at 307 nm and by the shoulder at 345 nm, which were consistent with the reported¹⁶ values for $\text{Pt}_2(\text{pop})_4\text{Br}_2^{4-}$, $\lambda_{\text{max}} (\epsilon) = 305$ nm ($55\,400$ L mol⁻¹ cm⁻¹), 345 nm ($11\,780$ L mol⁻¹ cm⁻¹). Also these peaks had the same absorbance ratio, $\Delta A_{307}/\Delta A_{345} = 4.8 \pm 0.3$, as the above molar absorptivities, $\epsilon_{305}/\epsilon_{345} = 4.7$. The apparent peak at 395 nm arises from convolution of the bleaching of the 369 nm $\text{Pt}_2(\text{pop})_4^{4-}$ band and the tail of the 345 nm absorption shoulder. This is supported by comparing the ratio of A_{345}/A_{395} found in this experiment (0.61) with that calculated from published¹⁷ spectra (0.60). Finally, the amount of product formed based on the analysis above is equal to the amount of reactant $\text{Pt}_2(\text{pop})_4^{4-}$ consumed, $(\Delta A/\epsilon)\text{Pt}_2(\text{pop})_4\text{Br}_2^{4-} \approx (\Delta A/\epsilon)\text{Pt}_2(\text{pop})_4^{4-}$. It can be concluded that ${}^3\text{Pt}_2(\text{pop})_4^{4-}$ is quenched by $\text{Co}(\text{CN})_5\text{Br}^{3-}$

(15) Kolthoff, I. M.; Khalafalla, S. E. In *Modern Aspects of Polarography*; T. Kambara, Ed.; Plenum Press: New York, 1966.

(16) Bryan, S. A.; Dickson, M. K.; Roundhill, D. M. *Inorg. Chem.* **1987**, *26*, 3878–3886.

(17) Dickson, M. K. Ph.D. Thesis, Washington State University, 1982.

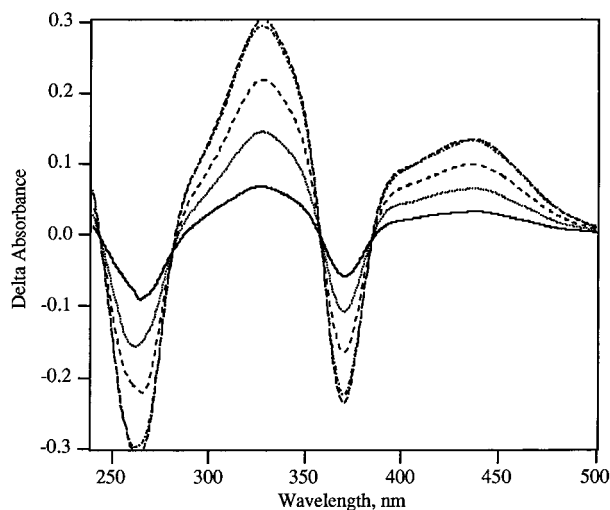
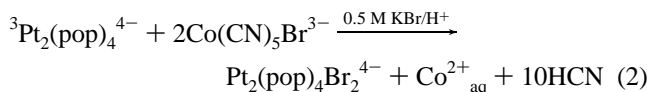
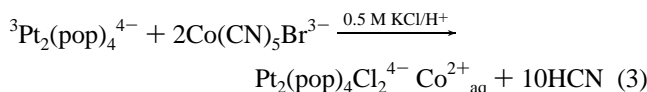


Figure 4. Absorbance change on photoreaction of ${}^3\text{Pt}_2(\text{pop})_4^{4-}$ with $\text{Co}(\text{CN})_5\text{I}^{3-}$ in 0.50 M KCl/0.010 M HClO_4 solution; Hg lamp, irradiation times: 30 s (—); 60 s (···); 90 s (---); 120 s (— · —); and kept in dark for 120 s after the last irradiation (— — —) (last two almost coincide).

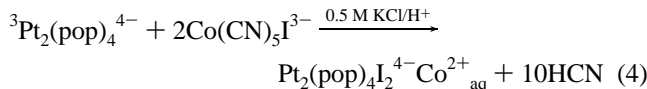
in a 0.5 M KBr medium to form the oxidation product, $\text{Pt}_2(\text{pop})_4\text{Br}_2^{4-}$, as shown in stoichiometric eq 2:



This equation has been written to show the final product of any initially formed $\text{Co}^{\text{II}}(\text{CN})_5$ species as $\text{Co}^{2+}_{\text{aq}}$ (plus HCN); destruction of such species will be rapid in these acidic solutions.¹⁸ When 0.50 M KCl was used as the electrolyte in the same reaction, i.e., X = Br but Y = Cl, the product was different, $\text{Pt}_2(\text{pop})_4\text{Cl}_2^{4-}$, not $\text{Pt}_2(\text{pop})_4\text{Br}_2^{4-}$, as shown in Figure 3. The absorption bands at 283 and 338 nm are reasonably consistent with the reported¹⁶ $\lambda_{\text{max}} = 282 \text{ nm}$ ($5 \times 10^4 \text{ L mol}^{-1} \text{ cm}^{-1}$), 345 nm ($7 \times 10^3 \text{ L mol}^{-1} \text{ cm}^{-1}$), and $\Delta A_{283}/\Delta A_{338} = 5.7 \pm 0.3$, close to the molar absorptivity ratio of 5.6. The amount of $\text{Pt}_2(\text{pop})_4\text{Cl}_2^{4-}$ formed is equal to the amount of $\text{Pt}_2(\text{pop})_4^{4-}$ consumed, $(\Delta A/\epsilon)_{\text{Pt}_2(\text{pop})_4\text{Cl}_2^{4-}} : (\Delta A/\epsilon)_{\text{Pt}_2(\text{pop})_4^{4-}} = 1.1 \pm 0.1$, as expected from eq 3.



In contrast to the above behavior, when $\text{Co}(\text{CN})_5\text{I}^{3-}$ was used as a quencher in a 0.5 M chloride medium (X = I, Y = Cl), the main quenching product was found to be $\text{Pt}_2(\text{pop})_4\text{I}_2^{4-}$ (Figure 4). New product peaks appeared at 328 and 438 nm; literature¹⁶ values for $\text{Pt}_2(\text{pop})_4\text{I}_2^{4-}$, $\lambda_{\text{max}} (\epsilon) = 331 \text{ nm}$ ($4 \times 10^4 \text{ L mol}^{-1} \text{ cm}^{-1}$), 438 nm ($1.7 \times 10^4 \text{ L mol}^{-1} \text{ cm}^{-1}$); experimental absorbance ratio, $A_{328}/A_{438} = 2.2$; literature $\epsilon_{331}/\epsilon_{438} = 2.4$, and $(\Delta A/\epsilon)_{\text{Pt}_2(\text{pop})_4\text{I}_2^{4-}} : (\Delta A/\epsilon)_{\text{Pt}_2(\text{pop})_4^{4-}} = 1.0 \pm 0.1$, consistent with eq 4.



However, Figure 4 shows that the peaks generated were accompanied by a high-energy shoulder, indicating some

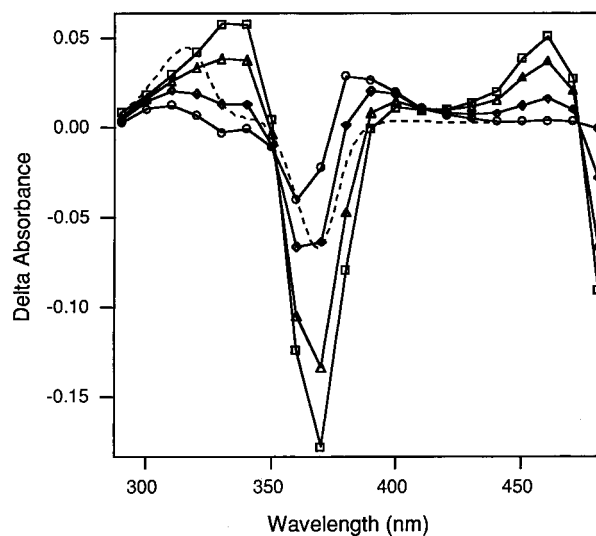


Figure 5. Transient absorbance changes after laser excitation (5 mJ at 355 nm) of $6 \times 10^{-5} \text{ M Pt}_2(\text{pop})_4^{4-}$ with $3.1 \times 10^{-4} \text{ M Co}(\text{CN})_5\text{I}^{3-}$ in 0.50 M $\text{NH}_4\text{ClO}_4/0.010 \text{ M HClO}_4$ solution. Delay times (in μs) are (\square) 0.7, (\triangle) 2.3, (\diamond) 6.5, and (\circ) 16. The dashed line shows the transient difference spectrum for $\text{Pt}^{\text{II}}\text{Pt}^{\text{III}}(\text{pop})_4(\text{H}_2\text{O})^{3-}$.

formation of side product(s). The shoulders near 282 and 345 nm are as one would expect for a small contribution of $\text{Pt}_2(\text{pop})_4\text{Cl}_2^{4-}$ [$\lambda_{\text{max}} (\epsilon) = 282 \text{ nm}$ ($5 \times 10^4 \text{ L mol}^{-1} \text{ cm}^{-1}$), 345 nm ($7 \times 10^3 \text{ L mol}^{-1} \text{ cm}^{-1}$)].¹⁶ Another possible side product is $\text{Pt}_2(\text{pop})_4\text{ClI}^{4-}$ [$\lambda_{\text{max}} (\epsilon) = 313 \text{ nm}$ ($4.1 \times 10^4 \text{ L mol}^{-1} \text{ cm}^{-1}$), 430 nm ($1.0 \times 10^4 \text{ L mol}^{-1} \text{ cm}^{-1}$)]. These absorption bands lie between those of $\text{Pt}_2(\text{pop})_4\text{Cl}_2^{4-}$ and $\text{Pt}_2(\text{pop})_4\text{I}_2^{4-}$ and are likely to be buried under them.

Unfortunately, experiments cannot be carried out in bulk KI as I^- quenches¹⁹ ${}^3\text{Pt}_2(\text{pop})_4^{4-}$ reductively in aqueous solution with a quenching rate constant $\log k_q = 5.7$.

The product quantum yields were measured using steady-state irradiation at 365 nm and found to be 0.027 ± 0.002 for the reaction between ${}^3\text{Pt}_2(\text{pop})_4^{4-}$ and $\text{Co}(\text{CN})_5\text{Br}^{3-}$ in 0.50 M KCl/pH 2 media, and 0.083 ± 0.002 for the reaction between ${}^3\text{Pt}_2(\text{pop})_4^{4-}$ and $\text{Co}(\text{CN})_5\text{I}^{3-}$ in 0.50 M KCl/pH 2, both with $(1-2) \times 10^{-4} \text{ M}$ quencher.

Laser Flash Transient Spectroscopy. Iodopentacyanocobaltate. Figure 5 shows the transient absorbance changes seen after a 5 mJ, 355 nm laser flash excitation of $\text{Pt}_2(\text{pop})_4^{4-}$ in the presence of sufficient $\text{Co}(\text{CN})_5\text{I}^{3-}$ to quench the emission lifetime by about 30% ($\sim 3 \times 10^{-4} \text{ M}$). Also shown for comparison purposes as the dashed line is the difference spectrum of the mixed-valence species $\text{Pt}^{\text{II}}\text{Pt}^{\text{III}}(\text{pop})_4(\text{H}_2\text{O})^{3-}$. The bleaching of ground-state $\text{Pt}_2(\text{pop})_4^{4-}$ at 368 nm and the transient absorption of ${}^3\text{Pt}_2(\text{pop})_4^{4-}$ at 460 and 330 nm can be seen at the earliest times (squares, triangles). These absorption changes decay with reasonable isosbestic points and with the quenched triplet lifetime. At the latest time shown in Figure 5 (circles), the ${}^3\text{Pt}_2(\text{pop})_4^{4-}$ has disappeared and the transient difference spectrum of the products of the quenching remains. Comparing this spectrum to the early time bleach of the $\text{Pt}_2(\text{pop})_4^{4-}$ absorption band shows clearly that a new absorption band has grown in at around 370–390 nm. The actual product spectrum is shown more clearly in Figure 6 (solid line), which is the spectrum calculated by adding back the ground-state $\text{Pt}_2(\text{pop})_4^{4-}$ spectrum to remove the ground-state bleaching effect. Figure 6 also shows spectra for the intermediates

(18) Espenson, J. H.; Pipal, J. R. *Inorg. Chem.* **1968**, *7*, 1463–1465.

(19) Roundhill, D. M.; Shen, Z.-P.; King, C.; Atherton, S. J. *J. Phys. Chem.* **1988**, *92*, 4088–4094.

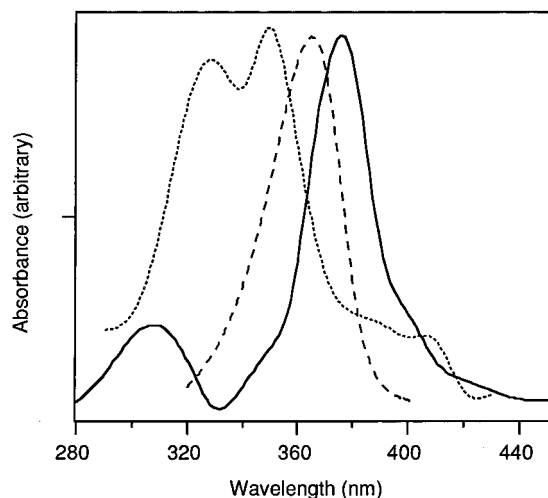


Figure 6. Calculated spectrum, solid line, of the transient present after the reaction in Figure 5. The dotted and dashed lines are the literature spectra for $\text{Pt}^{\text{II}}\text{Pt}^{\text{III}}(\text{pop})_4\text{Cl}^{4-}$ and $\text{Pt}^{\text{II}}\text{Pt}^{\text{III}}(\text{pop})_4\text{Br}^{4-}$, respectively.

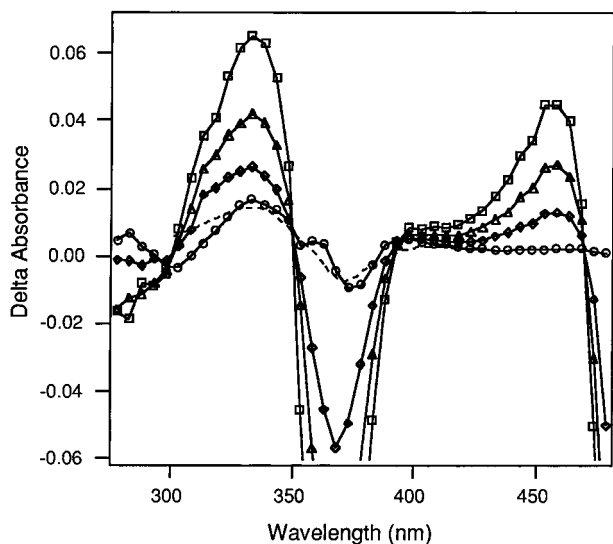


Figure 7. Transient absorbance changes during the first 20 μs after laser excitation (5 mJ at 355 nm) of 5×10^{-5} M $\text{Pt}_2(\text{pop})_4^{4-}$ with 1.9×10^{-3} M $\text{Co}(\text{CN})_5\text{Br}^{3-}$ in 0.50 M $\text{NH}_4\text{ClO}_4/0.010$ M HClO_4 solution. Delay times (in μs) are (\square) 0.5, (\triangle) 2, (\diamond) 4.4, and (\circ) 15. The dashed line is the transient difference spectrum reported for $\text{Pt}^{\text{II}}\text{Pt}^{\text{III}}(\text{pop})_4\text{Br}^{4-}$.

$\text{Pt}^{\text{II}}\text{Pt}^{\text{III}}(\text{pop})_4\text{Cl}^{4-}$ (dotted line) and $\text{Pt}^{\text{II}}\text{Pt}^{\text{III}}(\text{pop})_4\text{Br}^{4-}$ (dashed line), reported^{3-5,20} to be formed in the reaction of ${}^3\text{Pt}_2(\text{pop})_4^{4-}$ with RCl and RBr.

Bromopentacyanocobaltate. Figure 7 shows the time evolution of the transient absorption difference spectrum for 1.5×10^{-3} M $\text{Co}(\text{CN})_5\text{Br}^{3-}$ plus 5×10^{-5} M $\text{Pt}_2(\text{pop})_4^{4-}$ in a 0.5 M $\text{NH}_4\text{ClO}_4/1 \times 10^{-2}$ M HClO_4 medium at a pulse energy of 5 mJ at 355 nm. Under these circumstances, $\sim 50\%$ of the ${}^3\text{Pt}_2(\text{pop})_4^{4-}$ is quenched by the $\text{Co}(\text{CN})_5\text{Br}^{3-}$ both by calculation from the quenching rate constant measured⁶ earlier and from the observed ${}^3\text{Pt}_2(\text{pop})_4^{4-}$ phosphorescence lifetime decrease. First-order decay of the ${}^3\text{Pt}_2(\text{pop})_4^{4-}$ with good isosbestic points yields a transient difference spectrum which is compared in Figure 7 with the literature^{3-5,20} $\text{Pt}^{\text{II}}\text{Pt}^{\text{III}}(\text{pop})_4\text{Br}^{4-}$ spectrum. At longer times, the experimental spectrum evolves as shown in Figure 8, forming $\text{Pt}_2^{\text{III}}(\text{pop})_4\text{Br}^{4-}$ product with the difference spectrum shown earlier in Figure 3 (where the medium was

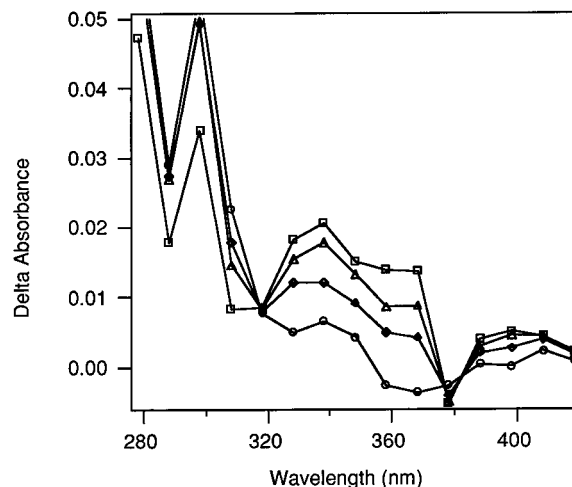


Figure 8. Transient absorbance changes at longer times after laser excitation (5 mJ at 355 nm) of 4.9×10^{-5} M $\text{Pt}_2(\text{pop})_4^{4-}$ with 2.5×10^{-3} M $\text{Co}(\text{CN})_5\text{Br}^{3-}$ in 0.50 M $\text{NH}_4\text{ClO}_4/0.010$ M HClO_4 solution. Delay times (in ms) are (\square) 0.3, (\triangle) 1.8, (\diamond) 3.8, and (\circ) 15.

KBr not NH_4ClO_4). The kinetics of this decay are available as Figure S2 in the Supporting Information. It is better fit by a second-order ($\chi^2 = 4 \times 10^{-5}$) than a first-order ($\chi^2 = 6 \times 10^{-5}$) decay curve, but the difference is largely obscured by the experimental noise. Also one obtains decreasing second-order rate constants for the decay when measured on progressively longer time scales, suggesting a distribution of second-order processes with different rate constants. This likely arises because of the inhomogeneous distribution of the intermediate produced in the laser and analyzing beam intersection region, resulting from its complex geometry.

Transient spectral studies on the $\text{Pt}_2(\text{pop})_4^{4-}/\text{Co}(\text{CN})_5\text{Br}^{3-}$ system were also carried out in KCl and KClO_4 but at much higher laser pulse energies where significant amounts of $\text{Pt}^{\text{II}}\text{Pt}^{\text{III}}(\text{pop})_4(\text{H}_2\text{O})^{3-}$ and solvated electron production occurred, roughly 50%. Under these conditions an alternative redox mechanism is possible via solvated electron/hydrogen atom reduction of the cobalt(III) complex accompanied by $\text{Pt}^{\text{II}}\text{Pt}^{\text{III}}(\text{pop})_4(\text{H}_2\text{O})^{3-}$ scavenging by halide ion available from the bulk or produced by decomposition of the reduced cobalt complex. The value of these experiments was that they showed that in 0.5 M KCl, $\text{Pt}^{\text{II}}\text{Pt}^{\text{III}}(\text{pop})_4(\text{H}_2\text{O})^{3-}$ forms $\text{Pt}^{\text{II}}\text{Pt}^{\text{III}}(\text{pop})_4\text{Cl}^{4-}$ by reaction with chloride ion within the decay lifetime of the doublet state, so that the transient spectrum obtained, available as supplementary Figure S3, is the same as that obtained by flashing $\text{Pt}_2(\text{pop})_4^{4-}$ alone in 0.5 M KCl (and notably different from the spectrum in water or 0.5 M NH_4ClO_4 shown in Figure 5). This intermediate decays with good second-order kinetics to produce the $\text{Pt}_2(\text{pop})_4\text{Cl}_2^{4-}$ product observed under these conditions.

In contrast, in 0.14 M KClO_4 where quenching is much less efficient, the spectrum of $\text{Pt}^{\text{II}}\text{Pt}^{\text{III}}(\text{pop})_4(\text{H}_2\text{O})^{3-}$ is distinctly seen at the end of the triplet decay, and this species then scavenges a bromide ion (available from the concomitant decomposition of $\text{Co}(\text{CN})_5\text{Br}^{3-}$) in a first-order process with a lifetime in the range 0.1–0.2 ms at the typical component concentrations present, forming $\text{Pt}^{\text{II}}\text{Pt}^{\text{III}}(\text{pop})_4\text{Br}^{4-}$ and eventually $\text{Pt}_2(\text{pop})_4\text{Br}_2^{4-}$. The significance of these observations is that when $\text{Pt}^{\text{II}}\text{Pt}^{\text{III}}(\text{pop})_4\text{Br}^{4-}$ is formed via the photoionization and bromide-scavenging mechanism, its formation is at least an order of magnitude slower than was observed in Figure 7.

Chloropentacyanocobaltate. Analogous behavior was found for $\text{Co}(\text{CN})_5\text{Cl}^{3-}$. Here a 5 mJ pulse at 355 nm excited

(20) Che, C.-M.; Gray, H. B.; Atherton, S. J.; Lee, W.-M. *J. Phys. Chem.* **1986**, *90*, 6747–6749.

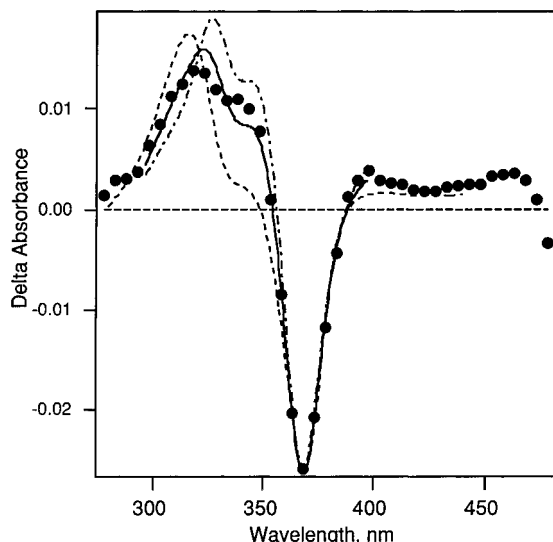


Figure 9. Difference spectrum (●) of the transient present after decay of triplet $\text{Pt}_2(\text{pop})_4^{4-}$ with $\text{Co}(\text{CN})_5\text{Cl}^{3-}$ in 0.50 M $\text{NH}_4\text{ClO}_4/0.010$ M HClO_4 solution, excited by a 5 mJ pulse at 355 nm. Dotted and dashed lines are the difference spectra for $\text{Pt}^{\text{II}}\text{Pt}^{\text{III}}(\text{pop})_4\text{Cl}^{4-}$ (literature⁴⁴) and $\text{Pt}^{\text{II}}\text{Pt}^{\text{III}}(\text{pop})_4(\text{H}_2\text{O})^{3-}$ (this work), and the solid line is a 60:40 mixture of these, respectively. The left absorbance scale applies to the data points; the spectra are in arbitrary units and have been scaled to match the experimental ground-state bleaching.

4.9×10^{-5} M $\text{Pt}_2(\text{pop})_4^{4-}$ in 0.5M $\text{NH}_4\text{ClO}_4/0.01\text{M}$ HClO_4 in the presence of 2.5×10^{-3} M $\text{Co}(\text{CN})_5\text{Cl}^{3-}$, sufficient to quench 25% of the $^3\text{Pt}_2(\text{pop})_4^{4-}$ excited states. First-order decay of the triplet left the difference spectrum which is compared in Figure 9 with the difference spectra for $\text{Pt}^{\text{II}}\text{Pt}^{\text{III}}(\text{pop})_4\text{Cl}^{4-}$ and for $\text{Pt}^{\text{II}}\text{Pt}^{\text{III}}(\text{pop})_4(\text{H}_2\text{O})^{3-}$. Also shown is a composite spectrum of a 60:40 mixture of these two spectra which, within the absorbance uncertainties, is a reasonable match to the observed spectrum.

Azidopentacyanocobaltate. $\text{Co}(\text{CN})_5\text{N}_3^{3-}$ showed quenching behavior that was very parallel to that for $\text{Co}(\text{CN})_5\text{I}^{3-}$. However, after the $^3\text{Pt}_2(\text{pop})_4^{4-}$ has decayed, the difference spectrum leads to a spectrum for the “intermediates” shown in Figure 10.

Experimental efforts to obtain a difference spectrum for the putative intermediate $\text{Pt}^{\text{II}}\text{Pt}^{\text{III}}(\text{pop})_4\text{N}_3^{4-}$ by generating $\text{Pt}^{\text{II}}\text{Pt}^{\text{III}}(\text{pop})_4(\text{H}_2\text{O})^{3-}$ in the presence of free azide ion were defeated because free azide is an extremely efficient quencher of $^3\text{Pt}_2(\text{pop})_4^{4-}$. This was not further investigated.

Discussion

General Comments. As has been discussed in our earlier paper,⁶ $\text{Co}(\text{CN})_6^{3-}$ did not quench $^3\text{Pt}_2(\text{pop})_4^{4-}$ (in reality $k_q < 10^6 \text{ M}^{-1} \text{ s}^{-1}$, based on the $\pm 0.1 \mu\text{s}$ uncertainty of the lifetime measurements). For the acidopentacyanocobaltate quenchers studied, the quenching rate constants were in the nearly diffusion-controlled regime, 10^7 – $10^8 \text{ L mol}^{-1} \text{ s}^{-1}$, decreasing in the order $\text{Co}(\text{CN})_5\text{I}^{3-} > \text{Co}(\text{CN})_5\text{N}_3^{3-} > \text{Co}(\text{CN})_5\text{Br}^{3-} > \text{Co}(\text{CN})_5\text{Cl}^{3-}$. In addition there are strong salt and specific cation effects associated with the quenching of $^3\text{Pt}_2(\text{pop})_4^{4-}$ by these complexes. This quenching could involve energy, electron, or atom transfer, of which the last process has been observed⁵ in quenching of $^3\text{Pt}_2(\text{pop})_4^{4-}$ by aromatic halides.

The choice between energy-transfer and electron-transfer mechanisms can be difficult in systems where there is no net reaction. Fortunately, the results presented here clearly demonstrate net photoredox reaction on quenching of $^3\text{Pt}_2(\text{pop})_4^{4-}$

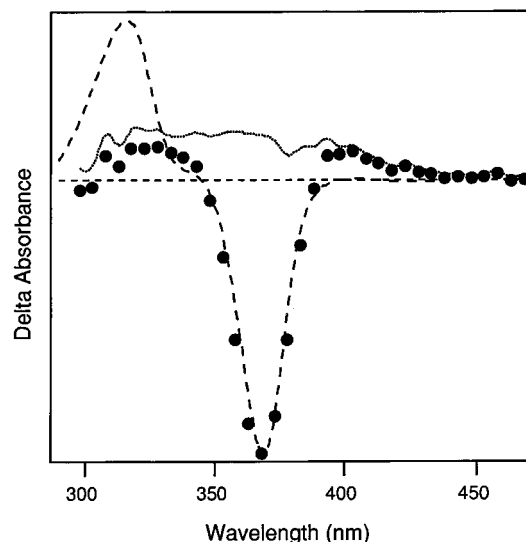


Figure 10. Difference spectrum (●) of the transient present after decay of triplet $\text{Pt}_2(\text{pop})_4^{4-}$ with $\text{Co}(\text{CN})_5\text{N}_3^{3-}$ in 0.50 M $\text{NH}_4\text{ClO}_4/0.010$ M HClO_4 solution, excited by a 5 mJ pulse at 355 nm. Dashed line is the difference spectrum expected for electron transfer; dotted line is the calculated spectrum of the products present (at 8 μs).

by these acidopentacyanocobaltate complexes. This is interesting and quite unusual as most studies of electron-transfer quenching involving $^3\text{Pt}_2(\text{pop})_4^{4-}$ and various quenchers have shown very rapid subsequent back electron transfer with no net redox products. It is fortunate because, given the information available, a choice between energy transfer and electron transfer on energetic grounds would be impossible.

Energy Transfer. For efficient energy transfer to take place, the excited-state energies of the quenchers $\text{Co}(\text{CN})_5\text{X}^{3-}$ should be lower than that of $^3\text{A}_{2u} \text{Pt}_2(\text{pop})_4^{4-}$. The latter triplet energy (E_t) has been estimated^{21–23} from the crossing points of the triplet absorption and emission bands to be $20.0 \pm 0.8 \text{ kK}$ ($\text{kK} = 10^3 \text{ cm}^{-1}$). Also $^3\text{Pt}_2(\text{pop})_4^{4-}$ can be quenched^{22,24} via energy transfer to anthracene ($E_t = 14.9 \text{ kK}$), $\text{Ru}(\text{bpy})_3^{2+}$ ($E_t = 16.9 \text{ kK}$), *trans*-stilbene ($E_t = 17.5 \text{ kK}$), and 1,3-cyclohexadiene ($E_t = 18.3 \text{ kK}$) with nearly diffusion-controlled quenching rate constants. For naphthalene ($E_t = 21.2 \text{ kK}$), the quenching rate constant falls 2 orders of magnitude below that of quenchers having $E_t < 17.7 \text{ kK}$ and 6 orders²² below that of biphenyl, which has $E_t = 23.0 \text{ kK}$. These quenching results support the spectroscopic value for the energy of $^3\text{Pt}_2(\text{pop})_4^{4-}$ ($^3\text{A}_{2u}$).

For $\text{Co}(\text{CN})_6^{3-}$, the $^3\text{T}_{1g}$ phosphorescence is at 14 kK in solids at low temperature.^{25–31} The location of the absorption band of the $^1\text{A}_{1g} \rightarrow ^3\text{T}_{1g}$ transition is not trivial due to the extremely

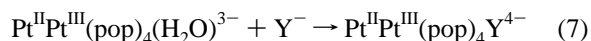
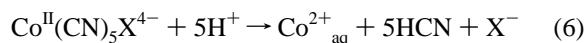
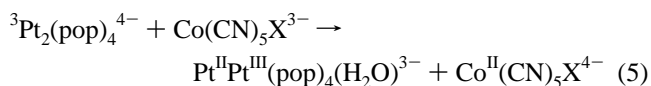
- (21) Fordyce, W. A.; Brummer, J. G.; Crosby, G. A. *J. Am. Chem. Soc.* **1981**, *103*, 7061–7064.
- (22) Peterson, J. R.; Kalyanasundaram, K. *J. Phys. Chem.* **1985**, *89*, 2486–2492.
- (23) Heuer, W. B.; Totten, M. D.; Rodman, G. S.; Hebert, E. J.; Tracy, H. J.; Nagle, J. K. *J. Am. Chem. Soc.* **1984**, *106*, 1163–1164.
- (24) Roundhill, D. M.; Shen, Z.-P.; Atherton, S. J. *Inorg. Chem.* **1987**, *26*, 3833–3835.
- (25) Mingardi, M.; Porter, G. B. *J. Chem. Phys.* **1966**, *44*, 4354.
- (26) Kirk, A. D.; Ludi, A.; Schlafer, H. L. *Ber. Bunsen Ges. Phys. Chem.* **1969**, *73*, 669–683.
- (27) Kirk, A. D.; Schlafer, H. L.; Ludi, A. *Can. J. Chem.* **1970**, *48*, 1065–1072.
- (28) Kataoka, H. *Bull. Chem. Soc. Jpn.* **1973**, *46*, 2078–2086.
- (29) Viaene, L.; D’Olieslager, J.; Ceulemans, A.; Vanquickenbourne, L. G. *J. Am. Chem. Soc.* **1979**, *101*, 1405–1409.
- (30) Mazur, U.; Hipps, K. W. *J. Phys. Chem.* **1980**, *84*, 194–197.
- (31) Wöpl, A.; Oelkrug, D. *Ber. Bunsen Ges. Phys. Chem.* **1975**, *79*, 394–400.

weak absorption,^{28,32} $\epsilon \approx 0.3-0.4$, for this spin-forbidden band. The energy was first claimed²⁵ to be 18.5 kK, but 24–27 kK has been suggested after more studies.^{26,28,29,31,33–35} Quenching data help clarify the situation. $\text{Co}(\text{CN})_6^{3-}$ can be sensitized by the excited state of biacetyl^{36,37} which has $E_t = 19.2-19.7$ kK,^{38,39} although the rate constant for quenching of biacetyl phosphorescence by $\text{Co}(\text{CN})_6^{3-}$ is very low at only $80 \text{ L mol}^{-1} \text{ s}^{-1}$. On the basis of this spectroscopic and quenching evidence, the triplet ${}^3\text{T}_{1g}$ of $\text{Co}(\text{CN})_6^{3-}$ has been suggested^{30,31,33,35,40} to be in the range of 18–20 kK and, therefore, slightly below ${}^3\text{Pt}_2(\text{pop})_4^{4-}$. Our observation that this complex does not quench ${}^3\text{Pt}_2(\text{pop})_4^{4-}$ is therefore useful; it suggests that either $\text{Co}(\text{CN})_6^{3-}$ has the higher excited triplet state energy or that factors such as a large internal reorganization energy are making energy transfer very slow as in the biacetyl example.

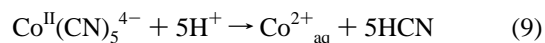
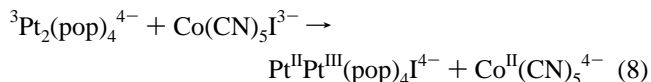
The energies of the lowest triplets of $\text{Co}(\text{CN})_5\text{X}^{3-}$ ($\text{X} = \text{I}, \text{N}_3, \text{Br}, \text{Cl}$) are not available spectroscopically because the phosphorescence has not been observed, but by ligand field expectations they should lie below the $\text{Co}(\text{CN})_6^{3-}$ complex. They may all therefore be thermodynamically capable of quenching the excited state ${}^3\text{Pt}_2(\text{pop})_4^{4-}$ via an energy-transfer process, giving ${}^3\text{Co}(\text{CN})_5\text{X}^{3-}$. However it has been found⁴¹ that these species are all rather poor quenchers of biacetyl triplets, again suggesting large reorganizational barriers to the process. It is highly unlikely that the “nearly diffusion-controlled” rate constants we observe arise in this manner. Also such energy-transfer processes could not lead to net redox reaction unless followed by electron transfer from excited cobalt complex to $\text{Pt}_2(\text{pop})_4^{4-}$. This is highly improbable given the nanosecond lifetimes expected for their triplet states based on the estimated 2.6 ns aqueous solution lifetime⁴² of ${}^3\text{Co}(\text{CN})_6^{3-}$. A convoluted energy/electron-transfer pathway for redox product formation can therefore be excluded, although we cannot entirely exclude some contribution from a parallel energy-transfer process.

Redox Quenching Mechanism. The observed values of $E_{1/2}$ for the four acidopentacyanocobaltate complexes of Table 1, together with $E(\text{Pt}_2(\text{pop})_4^{3-}/{}^3\text{Pt}_2(\text{pop})_4^{4-}) < -1.5 \text{ V}$ vs SCE in H_2O ,²³ show that all are thermodynamically able to oxidatively quench excited-state $\text{Pt}_2(\text{pop})_4^{4-}$, while this is unlikely with the poorer oxidant $\text{Co}(\text{CN})_6^{3-}$. Consistent with this, oxidized platinum photoproducts were observed only with the former complexes.

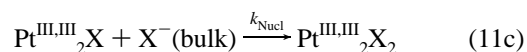
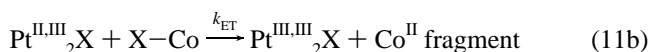
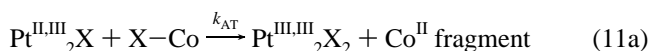
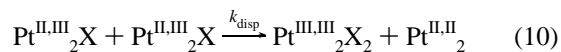
Thus when ${}^3\text{Pt}_2(\text{pop})_4^{4-}$ was quenched under steady-state conditions by $\text{Co}(\text{CN})_5\text{Br}^{3-}$ in a KBr or KCl medium, the photoproduct was $\text{Pt}_2(\text{pop})_4\text{Br}_2^{4-}$ or $\text{Pt}_2(\text{pop})_4\text{Cl}_2^{4-}$, respectively. This seemed to imply a primary electron transfer between ${}^3\text{Pt}_2(\text{pop})_4^{4-}$ and $\text{Co}(\text{CN})_5\text{X}^{3-}$ to form the unstable Co^{II} species and the mixed-valence $\text{Pt}^{\text{II}}\text{Pt}^{\text{III}}(\text{pop})_4(\text{H}_2\text{O})^{3-}$. The nucleophile Y^- ($\text{Y} = \text{Br}, \text{Cl}$), present in large excess in the medium, can then attack at the coordinately unsaturated Pt^{III} center, generating $\text{Pt}^{\text{II}}\text{Pt}^{\text{III}}(\text{pop})_4\text{Y}^{4-}$ (see eqs 5–7).



In contrast to this, when $\text{Co}(\text{CN})_5\text{I}^{3-}$ was the quencher in 0.5 KCl medium, the main product was $[\text{Pt}_2^{\text{III}}(\text{pop})_4\text{I}_2]^{4-}$ despite the availability of large amounts of chloride ion. This strongly implies that in this system the primary step is an atom-transfer process to give a reasonably substitutionally inert $\text{Pt}^{\text{II}}\text{Pt}^{\text{III}}(\text{pop})_4\text{I}^{4-}$ intermediate (eqs 8 and 9).



Primary steps 5 and 8 can clearly be distinguished if the platinum dimer intermediates $\text{Pt}^{\text{II}}\text{Pt}^{\text{III}}(\text{pop})_4(\text{H}_2\text{O})^{3-}$ and $\text{Pt}^{\text{II}}\text{Pt}^{\text{III}}(\text{pop})_4\text{I}^{4-}$ can be identified by transient spectroscopy. There is also an ambiguity about the pathway of formation of the final Pt(III) dimer product; this could be by disproportionation, reaction 10, of the $\text{Pt}^{\text{II}}\text{Pt}^{\text{III}}(\text{pop})_4\text{X}^{4-}$ intermediate ($\text{X} = \text{Cl}, \text{Br}, \text{I}$), symbolized as $\text{Pt}^{\text{II,III}}\text{X}$ in the equations below, or by reaction with a second mole of cobalt complex either by atom transfer (AT), reaction 11a, or electron transfer (ET), 11b followed by 11c.



These mechanistic questions were explored by transient spectroscopy to examine the intermediates present and their kinetics.

Cage Escape Yields. The observed product quantum yields, ϕ_{product} , show that the oxidative quenching pathway is reasonably efficient and requires that escape of the initial redox fragments competes with back reaction. Assuming no bulk recombination of redox species occurs, $\phi_{\text{product}} = \phi_{\text{isc}}\eta_{\text{q}}\eta_{\text{ce}}$, where ϕ_{isc} is the intersystem crossing quantum yield, η_{q} is the quenching efficiency by the cobalt complex, and η_{ce} is the cage escape efficiency. The $\text{Pt}_2(\text{pop})_4^{4-}$ absorption irradiated is ${}^1\text{A}_{1g} \rightarrow {}^1\text{A}_{2u}$ which intersystem crosses to the corresponding triplet state ${}^3\text{A}_{2u}$ with a yield approaching unity,⁴³ i.e., $\phi_{\text{isc}} = 1.0$. Using $\eta_{\text{Q}} = k_{\text{Q}}\tau^0[\text{Q}]/(1 + k_{\text{Q}}\tau^0[\text{Q}])$, the cage escape efficiencies η_{ce} were calculated to be 0.21 for $\text{Co}(\text{CN})_5\text{Br}^{3-}$ quencher and 0.34 for

(32) Nishazawa, M.; Ford, P. C. *Inorg. Chem.* **1981**, *20*, 294–295.

(33) Miskowski, V. M.; Gray, H. B.; Wilson, R. B.; Solomon, E. I. *Inorg. Chem.* **1979**, *18*, 1410–1412.

(34) Vanquickenborne, L. G.; Hendrickx, M.; Postelmans, D.; Hyla-Kryspin, I.; Pierloot, K. *Inorg. Chem.* **1988**, *27*, 900–907.

(35) Kida, S.; Fujita, J.; Nakamoto, K.; Tsuchida, R. *Bull. Chem. Soc. Jpn.* **1958**, *31*, 79–87.

(36) Scandola, M. A.; Scandola, F. *J. Am. Chem. Soc.* **1972**, *94*, 1805–1810.

(37) Porter, G. B. *J. Am. Chem. Soc.* **1969**, *91*, 3980–3982.

(38) Murov, S. L.; Carmichael, I.; Hug, G. L. *Handbook of Photochemistry*, 2nd ed.; Marcel Dekker, Inc.: New York, 1993; p 420.

(39) Vlcek, J. A.; Gray, H. B. *J. Am. Chem. Soc.* **1987**, *109*, 286–287.

(40) Demas, J. N.; Addington, J. W. *J. Am. Chem. Soc.* **1976**, *98*, 5800–5806.

(41) Wrighton, M.; Bredesen, D.; Hammond, G. S.; Gray, H. B. *J. Chem. Soc., Chem. Commun.* **1972**, 1018–1019.

(42) Conti, C.; Castelli, F.; Forster, L. S. *J. Phys. Chem.* **1979**, *83*, 2371–2375.

(43) Horváth, O.; Stevenson, K. L. *Charge-Transfer Photochemistry of Coordination Compounds*; VCH Publishers, Inc.: New York, 1993; p 380.

$\text{Co}(\text{CN})_5\text{I}^{3-}$ in the 0.5 M KCl medium. These can be less than unity because back-reaction, quenching to the ground state, or energy transfer to $\text{Co}(\text{CN})_5\text{X}^{3-}$ may compete. Due to the impossibility of observing the emission of ${}^3\text{Co}(\text{CN})_5\text{X}^{3-}$ in room temperature solutions, this last possibility cannot be completely discounted.

Transient Spectroscopy: Electron versus Atom Transfer.

The preliminary implications of the steady-state work were that the primary step was atom transfer for $\text{Co}(\text{CN})_5\text{I}^{3-}$ but electron transfer for $\text{Co}(\text{CN})_5\text{Br}^{3-}$ and $\text{Co}(\text{CN})_5\text{Cl}^{3-}$. In addition, there was the ambiguity about the pathway of formation of the final photoproduct. These questions were therefore investigated via transient spectroscopy of the intermediates formed and their decay pathways.

A difficulty in these experiments was the ready excited-state absorption of ${}^3\text{Pt}_2(\text{pop})_4^{4-}$ which leads to photoionization to $\text{Pt}^{\text{II}}\text{Pt}^{\text{III}}(\text{pop})_4(\text{H}_2\text{O})^{3-}$ and solvated electrons; under our conditions the latter would rapidly form hydrogen atoms. Both e^-_{aq} and H atoms could reduce the Co(III) complexes, providing an alternative route to redox reaction giving oxidized platinum and reduced cobalt species. Because of the relatively strong absorption of the ${}^3\text{Pt}_2(\text{pop})_4^{4-}$ at 355 nm, photoionization occurs significantly even down to pulse energies of 1 mJ. An irradiation wavelength on the red side of the $\text{Pt}_2(\text{pop})_4^{4-}$ maximum, say 375 nm, would alleviate this problem to a certain extent, but such was not available. Consequently to explore whether, for any quencher, the primary process was electron transfer leading to $\text{Pt}^{\text{II}}\text{Pt}^{\text{III}}(\text{pop})_4(\text{H}_2\text{O})^{3-}$ or atom transfer leading to $\text{Pt}^{\text{II}}\text{Pt}^{\text{III}}(\text{pop})_4\text{X}^{4-}$, it was necessary to use the minimum pulse energy possible to minimize interference from photoionization. The energy range 2–5 mJ was therefore adopted for such spectral measurements. We found that at 1 mJ, about 2–3% of the $\text{Pt}_2(\text{pop})_4^{4-}$ bleached leads to $\text{Pt}^{\text{II}}\text{Pt}^{\text{III}}(\text{pop})_4(\text{H}_2\text{O})^{3-}$ and e^-_{aq} and at 5 mJ, just under 10%. It was also necessary to work at as high as possible a concentration of $[\text{Co}(\text{CN})_5\text{X}]^{3-}$ to maximize the ratio of quenching to photoionization to ensure that any $\text{Pt}^{\text{II}}\text{Pt}^{\text{III}}(\text{pop})_4(\text{H}_2\text{O})^{3-}$ observed did truly arise from electron transfer quenching and not from photoionization. Choice of such conditions permitted reasonable spectral studies of the primary processes. However the transients were sufficiently weak that it was impossible using such low-energy pulses to explore the fate of the $\text{Pt}^{\text{II}}\text{Pt}^{\text{III}}(\text{pop})_4\text{X}^{4-}$ intermediates, which react on a much slower time scale of tens of ms. Since experiments showed that, even in perchlorate media, any $\text{Pt}^{\text{II}}\text{Pt}^{\text{III}}(\text{pop})_4(\text{H}_2\text{O})^{3-}$ generated always evolved on a sub-millisecond time scale to $\text{Pt}^{\text{II}}\text{Pt}^{\text{III}}(\text{pop})_4\text{X}^{4-}$ by halide ion scavenging, higher pulse energies were used to follow the kinetics of the $\text{Pt}^{\text{II}}\text{Pt}^{\text{III}}(\text{pop})_4\text{X}^{4-}$ intermediates.

In an earlier paper, evidence was presented⁷ that for the iodo quencher, ${}^3\text{Pt}_2(\text{pop})_4^{4-}$ reacts directly with $\text{Co}(\text{CN})_5\text{I}^{3-}$ to form an intermediate which then forms $\text{Pt}_2^{\text{III}}(\text{pop})_4\text{I}_2^{4-}$ on a much longer time scale. This was shown to occur by disproportionation, since no further consumption of $\text{Co}(\text{CN})_5\text{I}^{3-}$ was involved in the reaction, consistent with eq 10 but not with eq 11a or b. We also found that decay curves of the $\text{Pt}^{\text{II}}\text{Pt}^{\text{III}}(\text{pop})_4\text{I}^{4-}$ intermediate at long times are more consistent with the second-order kinetics expected for eq 10, although first- and second-order kinetics are hard to distinguish given the noise levels on the small signals seen. Figure 5 shows the transient difference spectrum obtained for this intermediate. Note that it appears during the doublet decay with reasonable isosbestic points and that the spectrum is distinctly different from the spectrum of $\text{Pt}^{\text{II}}\text{Pt}^{\text{III}}(\text{pop})_4(\text{H}_2\text{O})^{3-}$, whose main absorption peak is at 310–315 nm, and whose difference spectrum taken from the

literature⁴⁴ (and confirmed here) has been included in Figure 5 as the dashed curve. This is clear evidence that the redox process is not electron transfer. The atom-transfer process is suggested by Figure 6, where the spectrum of the intermediate has been calculated by adding back the spectrum of $\text{Pt}_2(\text{pop})_4^{4-}$ to cancel the bleach, and the resultant is compared with the literature spectra of the $\text{Pt}^{\text{II}}\text{Pt}^{\text{III}}(\text{pop})_4\text{Br}^{4-}$ and $\text{Pt}^{\text{II}}\text{Pt}^{\text{III}}(\text{pop})_4\text{Cl}^{4-}$ intermediates. The fact that the main peaks for the three $\text{Pt}^{\text{II}}\text{Pt}^{\text{III}}(\text{pop})_4\text{X}^{4-}$ species form a nice progression with a red shift consistent with expectations from ligand field theory indicates that this really is the spectrum of $\text{Pt}^{\text{II}}\text{Pt}^{\text{III}}(\text{pop})_4\text{I}^{4-}$ and that the quenching is by atom transfer. The product spectrum shows an additional small absorption band around 300 nm. The wavelength is not quite correct for $\text{Pt}^{\text{II}}\text{Pt}^{\text{III}}(\text{pop})_4(\text{H}_2\text{O})^{3-}$ arising from some electron transfer or photoionization. It could be that this is part of the 280 nm absorption band⁴⁵ of $\text{Co}(\text{CN})_5^{3-}$, the other product expected from the atom transfer. Only the long-wavelength tail would be seen because of the strong absorption by the quencher below 300 nm which restricts the observational window.

For $\text{Co}(\text{CN})_5\text{Br}^{3-}$, Figure 7, similar ${}^3\text{Pt}_2(\text{pop})_4^{4-}$ decay with good isosbestic points is observed, and the resultant difference spectrum is a good match to that for $\text{Pt}^{\text{II}}\text{Pt}^{\text{III}}(\text{pop})_4\text{Br}^{4-}$ (dashed line). There is no significant additional absorption that could be attributed to $\text{Pt}^{\text{II}}\text{Pt}^{\text{III}}(\text{pop})_4(\text{H}_2\text{O})^{3-}$, so we conclude again that the primary process is atom transfer. Unfortunately the absorption of the $\text{Co}(\text{CN})_5\text{Br}^{3-}$ complex is too far into the UV to observe any bleaching of the Co complex, so we could not get direct proof that the intermediate decays by disproportionation rather than further reaction with Co complex. However, Figure 8 shows that the further reaction of $\text{Pt}^{\text{II}}\text{Pt}^{\text{III}}(\text{pop})_4\text{Br}^{4-}$ to $\text{Pt}_2(\text{pop})_4\text{Br}_2^{4-}$ occurs with good isosbestic points and the kinetic traces for this parallel those described for the iodo system, i.e., better second-order than first-order fits, but decreasing second-order rate constants when measured on longer time scales.

Figure 9 shows the similar atom transfer behavior observed with $\text{Co}(\text{CN})_5\text{Cl}^{3-}$ quencher, but now there is evidence in the shape of the product spectrum for some formation of $\text{Pt}^{\text{II}}\text{Pt}^{\text{III}}(\text{pop})_4(\text{H}_2\text{O})^{3-}$, indicative of electron-transfer quenching. As shown in the figure, a reasonable fit to the data is obtained for 60% $\text{Pt}^{\text{II}}\text{Pt}^{\text{III}}(\text{pop})_4\text{Cl}^{4-}$ and 40% $\text{Pt}^{\text{II}}\text{Pt}^{\text{III}}(\text{pop})_4(\text{H}_2\text{O})^{3-}$. However this 60% figure is likely to be a lower limit; $\text{Co}(\text{CN})_5\text{Cl}^{3-}$ is the poorest quencher and likely has a lower cage escape yield than its analogues. Consequently any $\text{Pt}^{\text{II}}\text{Pt}^{\text{III}}(\text{pop})_4(\text{H}_2\text{O})^{3-}$ formed by photoionization is most noticeable for this system. We conclude that even for $\text{Co}(\text{CN})_5\text{Cl}^{3-}$, atom transfer is the dominant and possibly exclusive redox process.

$\text{Co}(\text{CN})_5\text{N}_3^{3-}$ gave results that were inconclusive. The spectrum for the “intermediates” shown in Figure 10 allows us to conclude definitely that the process involved is not simply electron transfer, as little or no $\text{Pt}^{\text{II}}\text{Pt}^{\text{III}}(\text{pop})_4(\text{H}_2\text{O})^{3-}$ is seen. However, there is no clear transient spectrum of a $\text{Pt}^{\text{II}}\text{Pt}^{\text{III}}(\text{pop})_4\text{N}_3^{4-}$ species analogous to that reported earlier⁴⁶ for $\text{Pt}^{\text{II}}\text{Pt}^{\text{III}}(\text{pop})_4\text{SCN}^{4-}$. The diffuse spectrum observed looks as if it is for a mixture of several species, and we conclude that this may be due to the strong oxidizing capability of azide, which probably leads to further rapid oxidation processes in the putative intermediate formed initially.

(44) Cho, K. C.; Che, C. M. *Chem. Phys. Lett.* **1986**, *124*, 313–316.

(45) King, N. K.; Winfield, M. E. *J. Am. Chem. Soc.* **1961**, *83*, 3366–3373.

(46) Che, C.-M.; Cho, K.-C.; Chan, W.-S.; Gray, H. B. *Inorg. Chem.* **1986**, *25*, 4906–4909.

Interconversion of Intermediates. If all three halopentacyano systems show primary atom transfer followed by disproportionation of $\text{Pt}^{\text{II}}\text{Pt}^{\text{III}}(\text{pop})_4\text{X}^{4-}$ to $\text{Pt}^{\text{II}}\text{Pt}^{\text{III}}(\text{pop})_4\text{X}_2^{4-}$, we need to explain the origins in the steady-state experiments of the minor amounts of $\text{Pt}_2(\text{pop})_4\text{ICl}^{4-}$ in the $\text{Co}(\text{CN})_5\text{I}^{3-}/\text{KCl}$ system and the $\text{Pt}_2(\text{pop})_4\text{Cl}_2^{4-}$ product in the $\text{Co}(\text{CN})_5\text{Br}^{3-}/\text{KCl}$ system. Given previous studies¹⁶ of substitution processes in platinum dimer systems, the obvious suggestion is an exchange process involving the mixed-valence intermediates (eq 12).



This could occur as written or could be catalyzed by $\text{Pt}_2(\text{pop})_4^{4-}$ analogously to the reported¹⁶ photocatalysis of halide exchange in $\text{Pt}_2(\text{pop})_4\text{X}_2^{4-}$. There, photochemically produced $\text{Pt}_2(\text{pop})_4^{4-}$ undergoes the reverse of the disproportionation process shown in reaction 10. For the more easily replaced bromide ion, this exchange needs to be rapidly completed in 0.5 M chloride, and this was supported by our observation that quenching by $\text{Co}(\text{CN})_5\text{Br}^{3-}$ in 0.5 M chloride gave the same difference spectrum after ${}^3\text{Pt}_2(\text{pop})_4^{4-}$ decay as was obtained by photoionizing $\text{Pt}_2(\text{pop})_4^{4-}$ in 0.5 M KCl. In contrast, the iodide ion bonds very strongly to platinum and may not be quickly replaced by chloride, allowing formation of only minor amounts of $\text{Pt}_2(\text{pop})_4\text{ICl}^{4-}$ in 0.5 M KCl. In support of these ideas, it has been shown that the stability of the mixed valence intermediate $\text{Pt}^{\text{II,III}}_2\text{X}$ increases⁴⁶ with increasing nucleophilicity of X ($\text{Cl}^- < \text{Br}^- < \text{I}^-$).

Conclusions

All three halopentacyanocobaltate(III) complexes oxidatively quench ${}^3\text{Pt}_2(\text{pop})_4^{4-}$ by atom transfer, while the mechanism with the azido analogue appears to be complex. The efficiency of atom transfer decreases from the iodo to the bromo complex and probably to the chloro complex. This can be rationalized in terms of three factors: excited-state ${}^3\text{Pt}_2(\text{pop})_4^{4-}$ has a strong

affinity for the “soft” iodo ligand,⁴⁷ the stability of the mixed-valence intermediate $\text{Pt}^{\text{II,III}}_2\text{X}$ increases⁴⁶ with increasing nucleophilicity of X ($\text{Cl}^- < \text{Br}^- < \text{I}^-$), and finally the bond dissociation energies, D°_{298} , for Co–Cl, Co–Br, and Co–I are 389, 331, and 285 kJ/mol, respectively,⁴⁸ indicating that the Co–I bond is much weaker than Co–Br or Co–Cl. Finally, the results observed here are consistent with literature findings⁴⁹ that the atom-transfer rates to ${}^3\text{Pt}_2(\text{pop})_4^{4-}$ from alkyl halides increase in the order $\text{RCl} < \text{RBr} < \text{RI}$. As far as we are aware, these $\text{Pt}_2(\text{pop})_4^{4-}/\text{Co}(\text{CN})_5\text{X}^{3-}$ systems represent the first examples of excited-state atom transfers between two coordination complexes. This likely reflects the 17-electron radical character of $\text{Co}(\text{CN})_5^{3-}$ and invites examination of analogous isolobal systems.

The results also imply that energy- and electron-transfer processes involving $\text{Co}(\text{CN})_5\text{X}^{3-}$ are slow. Because of the strong-field, low-spin character of the Co(III) starting materials, these processes are likely confronted by a large internal reorganizational energy barrier.

Acknowledgment. The authors thank J. Nagle and M. Roundhill for helpful discussions, L. Netter and C. Bohne for assistance with the laser flash system, and the Natural Sciences and Engineering Council of Canada and the University of Victoria for financial support.

Supporting Information Available: Figure S1, spectra of the acidopentacyanocobaltates complexes; Figure S2, kinetics of $\text{Pt}^{\text{II}}\text{Pt}^{\text{III}}(\text{pop})_4\text{Br}^{4-}$ decay; and Figure S3, transient difference spectrum for $\text{Pt}^{\text{II}}\text{Pt}^{\text{III}}(\text{pop})_4\text{Cl}^{4-}$ in 0.5 M KCl (3 pages). Ordering information is given on any current masthead page.

IC971096+

- (47) Roundhill, D. M. *Photochemistry and Photophysics of Metal Complexes*; Plenum Press: New York, 1994; p 356.
 (48) Weast, R. C.; Lide, D. R.; Astle, M. J.; Beyer, W. H. *CRC Handbook of Chemistry and Physics*, 70th ed.; CRC Press, Inc.: Boca Raton, FL, 1990.
 (49) Creutz, C.; Song, J.-S.; Bullock, R. M. *Pure Appl. Chem.* **1995**, *67*, 47–54.